Entropy of Li intercalation in Li_xCoO_2

Yvan Reynier,[1,2] Jason Graetz,[1] Tabitha Swan-Wood,[1] Peter Rez,[3] Rachid Yazami,[1,2] and Brent Fultz[1]
[1]*California Institute of Technology, W. M. Keck Laboratory, Pasadena, California 91125, USA*
[2]*CNRS (UMR5631)-BP75 38402 St. Martin d'Heres, France*
[3]*Department of Physics and Astronomy, Arizona State University, Tempe, Arizona 85287, USA*
(Received 26 February 2004; revised manuscript received 2 July 2004; published 17 November 2004)

The entropy of lithiation of Li_xCoO_2 for $0.5 < x \leqslant 1.0$ was determined from measurements of the temperature dependence of equilibrated voltages of electrochemical cells. Measured changes in the entropy of the lithiation reaction were as large as 9.0 k_B/atom, and as large as 4.2 k_B/atom within the "O3" layered hexagonal structure of Li_xCoO_2. Three contributions to the entropy of lithiation for the O3 phase were assessed by experiment and calculation. The phonon entropy of lithiation was determined from measurements of inelastic neutron scattering. Phonon entropy can account for much of the negative entropy of lithiation, but its changes with lithium concentration were found to be small. Electronic structure calculations in the local density approximation gave a small electronic entropy of lithiation of the O3 phase. The configurational entropy from lithium-vacancy disorder was large enough to account for most of the compositional trend in the entropy of lithiation of the O3 phase if ordered structures exist at lithium concentrations of $x=1/2$ and $x=5/6$. The electrochemical measurements showed the existence of a two-phase region in the composition range between $x=5/6$ and 0.95. Electronic structure calculations gave evidence that these phases were metallic and insulating, respectively. Changes of the electronic and configurational entropy were found to be of comparable importance for this metal-insulator transition.

DOI: 10.1103/PhysRevB.70.174304 PACS number(s): 65.40.Gr, 82.60.−s

I. INTRODUCTION

Entropy is central to the understanding of phase transitions and chemical reactions of materials. The statistical mechanics origin of entropy begins with the Boltzmann epitaph equation,

$$S = k_B \ln(W), \tag{1}$$

where W is the number of ways for obtaining equivalent states of the system, and k_B is the Boltzmannn constant. Equation (1) pertains to individual entities such as atoms, electrons, and phonons, once the configurations or states of these entities are enumerated by W. The challenge for understanding phase transitions and chemical reactions is to identify the physical sources of W, and evaluate it.

The chemical insertion of Li into the layered hexagonal phase of Li_xCoO_2 is a chemical reaction of technological importance because Li_xCoO_2 is widely used in cathodes of commercial rechargeable lithium batteries. A second reaction of Li extraction occurs at an anode. If these two reactions occur quasistatically, the voltage of the cell is the difference in chemical potential of the Li in the anode and the cathode, or the free energy per mole:

$$\Delta G = \Delta U - T\Delta S + P\Delta V, \tag{2}$$

$$\Delta G = -F\Delta E, \tag{3}$$

where F is the Faraday constant for converting between the amount of charge that passes across the voltage drop ΔE, and ΔG, the Gibbs free energy per mole. Here ΔU is the difference of internal energy for a mole of lithium in the anode and cathode, ΔV is the difference in specific volume associated with adding lithium to the anode and the cathode, T is temperature, and P is pressure. We will later use the difference in enthalpy, $\Delta H = \Delta U + P\Delta V$.

The temperature dependence of the voltage ΔE in Eq. (3) can be used to measure the entropy of the Li insertion reaction. Equating Eqs. (2) and (3), and differentiating with respect to T:

$$\Delta S = F\frac{\partial \Delta E}{\partial T}. \tag{4}$$

When the anode is pure bcc Li metal, the entropy or enthalpy per mole of lithium in the anode cannot change with the transfer of lithium from the anode to the cathode. Variations of the cell voltage with temperature reflect changes in the cathode alone and hence the temperature dependence of the open circuit voltage can be used to obtain the entropy of lithium intercalation into Li_xCoO_2 at different lithium concentrations, x. For a significant change in ΔS of order k_B per atom, the corresponding change $\partial\Delta E/\partial T$ is approximately 0.086 mV/K. This is of minor importance to the technology of the cell voltage. Nevertheless, these changes can be measured accurately over temperature ranges of several degrees K, and can be used as an accurate measure of the ΔS and other thermodynamic properties of the lithium insertion reaction in Li_xCoO_2.

Here we report large changes in the total entropy of the lithium insertion reaction in Li_xCoO_2 at different values of x. Magnetic entropy and nuclear entropy are not expected to vary with x. For Li_xCoO_2, the possible sources of entropy for Eq. (1) are as follows:

(1) configurational entropy, ΔS_{cf}, originating from the disorder of placing vacancies on the Li atom sites,

(2) phonon entropy, ΔS_{ph}, associated with a dependence

of vibrational frequencies on x (phonon entropy has been a topic of recent experimental[1–3] and theoretical[4–6] research), and

(3) electronic entropy, ΔS_{el}, associated with thermal disorder in electron states near the Fermi level.

These three contributions to the entropy of the lithiation reaction of the layered "O3" hexagonal phase of Li_xCoO_2 were assessed individually in the present research. The phonon density of states measurements by inelastic neutron scattering showed that the compositional trends of the phonon entropy were small, but phonon entropy can account for much of the negative values of the entropy of lithiation. Electronic structure calculations in the local density approximation showed that the electronic entropy of lithiation is negligible. Large variations of the configurational entropy were caused by changes in the lithium-vacancy disorder with x. A two-phase region exists from $x=0.833$ to $x=0.95$. Electronic structure calculations confirmed that this phase change involves a metal-insulator transition, for which the changes in electronic entropy and configurational entropy were of comparable magnitude.

II. EXPERIMENT

A. Sample preparation

The $LiCoO_2$ powders were prepared by Enax Inc. using a conventional synthesis method.[7] Spectral analysis of the powders (performed by ENAX) revealed less than 0.02 at% metal impurities (Cr, Fe, Ni, Cu, Al) and approximately 0.17 at% H_2O. The $LiCoO_2$ used in the electrochemical cells and the neutron experiments was a coarse-grained powder with a mean particle size of 13 μm and a surface area 0.33 m^2/g. Foil cathodes containing 91% active material were also provided by Enax, Inc.

The samples used in the inelastic neutron scattering experiments were prepared by chemical delithiation of $LiCoO_2$ powder. An aqueous solution containing a variable concentration of potassium persulfate ($K_2S_2O_8$) was used to extract lithium ions from the stoichiometric material. The oxidizing solution was heated to 60 °C and agitated for approximately 24 h. The delithiated samples were subsequently washed in distilled water, filtered, and dried in vacuum at 60 °C for 12 h. An Inel CPS-120 x-ray diffractometer with Co $K\alpha$ radiation was used to measure the crystal structure of the delithiated compounds. A compositional analysis was performed using the a and c lattice parameters, which have been shown to scale linearly with lithium concentration.[8] Thermal gravimetric analysis and mass spectrometry were used to determine the sample impurities. The delithiated samples evolved up to 4.5% of their original mass at temperatures of around 290 °C. The evolved compounds were determined to be predominately oxygen and water, indicating that the delithiated samples contain absorbed/adsorbed H_2O and OH groups ($\leqslant$4.5 wt%).

B. Electrochemical measurements

The open circuit voltage (OCV) of Li/Li_xCoO_2 half cells was measured as a function of temperature at various lithium concentrations to determine the entropy and enthalpy of the following reaction:

$$LiCoO_2 \Leftrightarrow Li_xCoO_2 + (1-x)Li, \quad 0.5 < x < 1. \qquad (5)$$

Coin cells of 20 mm diameter and 1.6 mm thickness with a metallic lithium counter electrode were assembled in an argon-filled glove box. The electrolyte (Mitsubishi Chemicals Co.) was a solution of molar $LiClO_4$ in polyethylene carbonate. Microporous polyethylene separators from the Tonen Co. were soaked overnight in the electrolyte before use. The cells were first cycled five times using an Arbin BT2000 cycler between 2.9 and 4.2 V vs. Li^+/Li at a C/10 rate (i.e., the electrodes went between full charge and full discharge in 10 h), corresponding to a current of 425 $\mu A/cm^2$. For the last charge the 4.2 V potential was maintained for 2 h. The OCV was monitored with an Arbin BT4+ while the temperature was decreased from room temperature to −3 °C in several steps using a Boekel Peltier Tropicooler. Between each OCV measurement the cells were discharged using the same C/10 rate, and allowed to equilibrate for at least 4 hours. Representative OCV data, shown in Fig. 1, were obtained in pairs to check the experiment reproducibility.

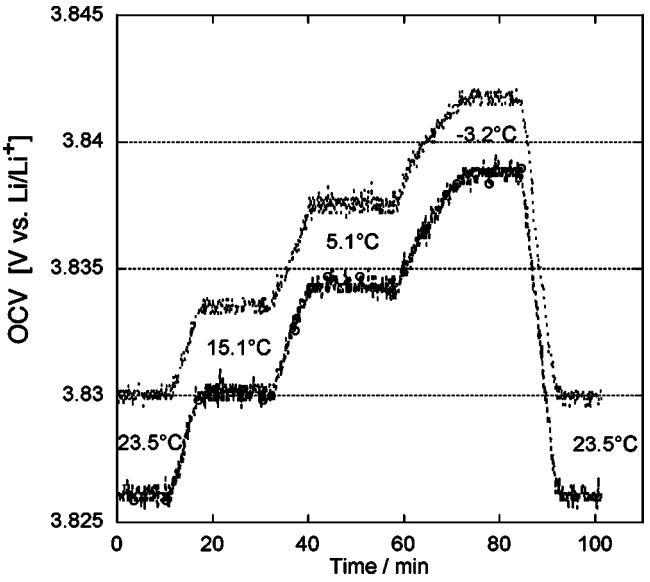

FIG. 1. Typical measurement of open-circuit voltage versus time for the fully lithiated lithium cobalt oxide. Results are shown for two cells.

C. Inelastic neutron scattering

Inelastic neutron spectra were acquired with the Pharos instrument, a time-of-flight chopper spectrometer at the Los Alamos Neutron Scattering Center, LANSCE, at the Los Alamos National Laboratory. The position sensitive detectors on Pharos cover an angular range of −10° to +140°. Independent sets of data were acquired from neutron beams having incident energies of 147 and 243 meV, corresponding to maximum momentum transfers of 20.1 and 25.8 $Å^{-1}$. All sample holders were machined aluminum cans of annular geometry with inner and outer wall thicknesses of 1.0 mm.

TABLE I. Samples of Li_xCoO_2 for neutron scattering, where x is lithium concentration. Values of S_{ph} are not corrected for the neutron weighting of the measured spectra.

x	ID(cm)	OD(cm)	ρ(g/cm^3)	$S_{ph}(k_B/\text{atom})$
1.00	4.884	5.080	2.35	1.25
0.76	4.846	5.080	2.34	1.24
0.62	4.813	5.080	2.11	1.35
0.58	4.788	5.080	2.20	1.26

Sample geometries were chosen to maximize scattering flux while minimizing absorption, and inner and outer diameters (ID and OD) were as listed in Table I.

The Li_xCoO_2 powder was packed loosely into the aluminum can and sealed with rubber O rings in an argon atmosphere. Spectra were acquired from empty aluminum cans under the same conditions as their corresponding samples to obtain appropriate background spectra. Measurements were performed at ambient pressure and room temperature.

D. Electronic structure calculations

The electronic structure calculations were performed with the ab-initio total energy and molecular dynamics program VASP (Vienna *ab initio* simulation program), which uses ultrasoft pseudopotentials.[9] Electronic structures for the ordered O3 structures of layered hexagonal Li_xCoO_2 taken from Van der Ven *et al.*[10] were calculated in the local density approximation. The structure for $x=0.916$ corresponding to $Li_{11}(CoO_2)_{12}$ was created in the same way. A triclinic cell was built up from stacked layers of Li, O and Co, each with 12 atoms. One Li atom was removed to give the desired stochiometry. The total energy was converged to 0.1 meV. Good agreement was found with previous results,[10] as expected. As the changes with stoichiometry were very small, it is expected that different structural models would not have significantly different densities of states. Because the structures were not simple cubic or hexagonal structures, the Gaussian smearing method[11] was used to calculate the density of states from the eigenvalues. The half-width of the Gaussian function was 25 meV to model the thermal spread. A check was made that sufficient k points had been included to achieve convergence.

III. RESULTS

A. Electrochemical measurements

The entropy of lithiation in Li_xCoO_2 versus lithium concentration, x, is presented in Fig. 2. By integration of the current passed through the cells, the lithium concentration was determined to vary from $x=0.49$ to 1.0. The entropy peak corresponding to the monoclinic transition is first observed at $x=0.55$ (descriptions of the different phases are provided at the start of the next section). This phase has significantly positive entropy, compared to the -20 J mol^{-1} K^{-1} of the layered hexagonal phase in the same region. Figure 3 shows that this order-disorder transition is also temperature dependent: for $x=0.55$, when the temperature is increased from 270 to 330 K, a clear change in the slope of the OCV vs T curve is observed, with two linear parts corresponding to the monoclinic and layered hexagonal phases. This result is in accordance with the previously determined phase diagrams.[8,10] A monotonic decrease is then observed from $x=0.6$ to 0.83, corresponding to the filling of Li sites in the layered hexagonal phase, followed by a plateau up to $x=0.95$, characteristic of the first-order phase transition between the metallic and semiconductor phases associated with vacancy arrangements. In the last region the entropy increases sharply. These results are in good agree-

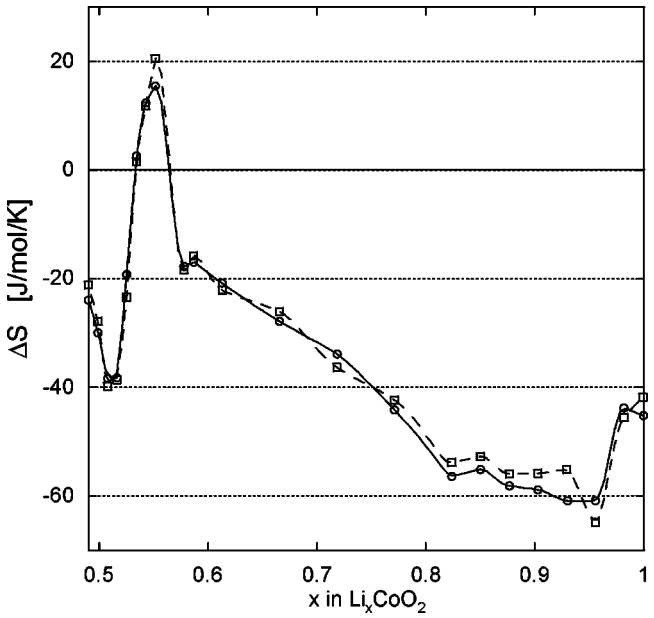

FIG. 2. Entropy of lithiation in Li_xCoO_2 versus Li concentration, x. Results are shown for two cells.

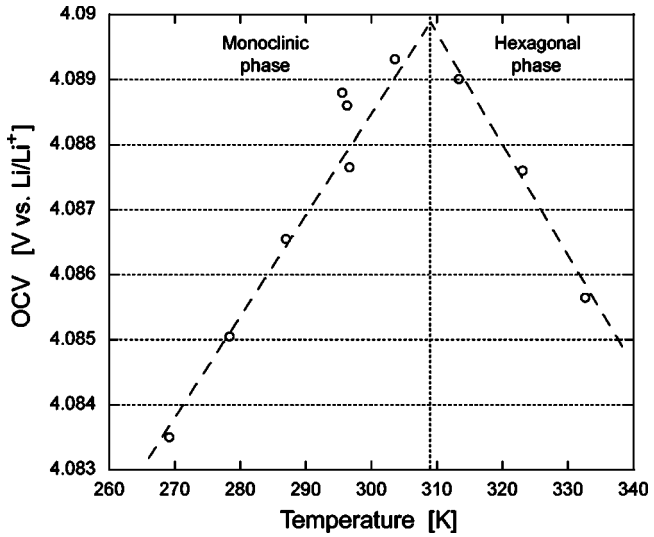

FIG. 3. Change of OCV versus temperature across the temperature range of the monoclinic to layered hexagonal transition at $T \simeq 309$ K, for $x=0.55$. The entropy from the slope of the dashed line for the monoclinic phase is +18 J/(mol K), whereas for the layered hexagonal phase it is -17 J/(mol K).

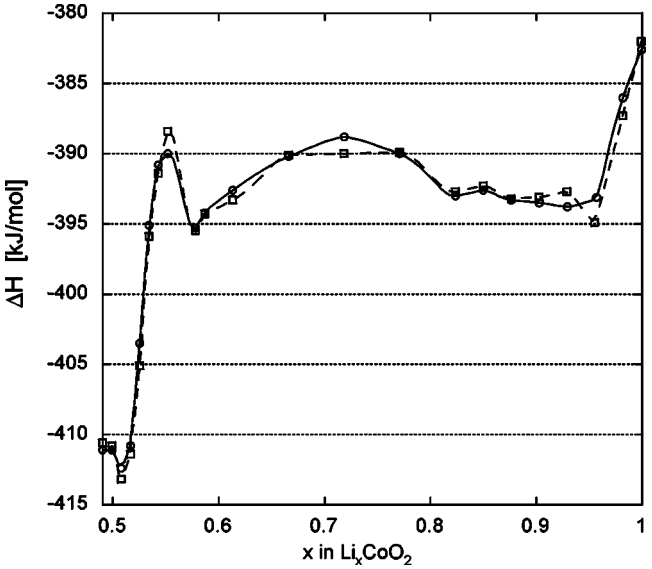

FIG. 4. Enthalpy of lithiation in Li_xCoO_2 versus Li concentration, x. Results are shown for two cells.

ment with those published by Thomas and Newman,[12] apart from the final range from $x=0.95$ to 1.0.

The enthalpy of lithiation (Fig. 4) also exhibits these four regions. Between $x=0.49$ and 0.58, the monoclinic transition is accompanied by a large enthalpy variation. The enthalpy then varies moderately in the single-phase layered hexagonal region up to $x=0.83$. The enthalpy of lithiation is nearly constant between $x=0.83$ and 0.95, consistent with a first-order transition in this region. Finally, a sharp increase is observed when the last empty Li sites are filled at large x.

B. Configurational entropy

The classical configurational entropy of mixing can be calculated in the point approximation with Eq. (1) for a fully disordered lattice of lithium atoms and vacant sites:

$$S_{cf}(x) = -k_B(x_2 - x_1)[\chi \ln \chi + (1-\chi)\ln(1-\chi)], \quad (6)$$

$$\chi \equiv \frac{x - x_1}{x_2 - x_1}, \quad (7)$$

where x_1 and x_2 are the lithium concentrations of stoichiometric structures that are modified by lithium atom-vacancy disorder when $x_1 < x < x_2$. The ΔS measured in the lithium insertion reaction is the derivative of $\Delta S_{cf}(x)$ with respect to x:

$$\frac{\Delta S_{cf}(x)}{\Delta x} = k_B \ln\left(\frac{1-\chi}{\chi}\right), \quad (8)$$

$$\frac{\Delta S_{cf}(x)}{\Delta x} = k_B \ln\left(\frac{x_2 - x}{x - x_1}\right). \quad (9)$$

Although this expression is singular at $x=x_1$ and $x=x_2$, the divergence is logarithmic and $\Delta S_{cf}(x)/\Delta x = \pm 4.6 k_B$/atom at $\chi=0.01$ or $\chi=0.99$, for example. The free parameters in Eq. (9) are the end point compositions x_1 and x_2. From the experimental results of Fig. 2 and 4, we can see that the two-phase region has a boundary at the concentration of $5/6 = 0.833$, which is the value of the endpoint composition x_2 for the metallic hexagonal phase. The other end point composition is less obvious from the experimental data, although previous work has reported an ordered composition at the composition of $x=0.5$, suggesting this is the compositional endpoint, x_1, for the hexagonal phase.[13] Ordered structures have been predicted at the temperature 300 K for other compositions between $x=0.5$ and $x=0.8333$.[14] In what follows, we tested several values for x_1 including 0.0 and 0.5.

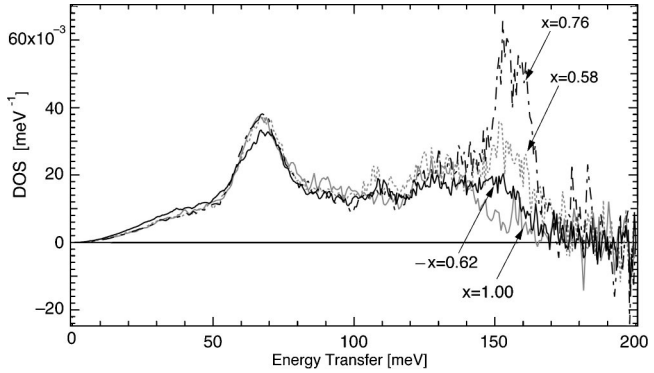

FIG. 5. Neutron-weighted DOS curves for incident energy of 243 meV. DOS curves have been normalized to unity up to 80 meV, ignoring the OH/H_2O vibrational modes around 150 meV.

C. Inelastic neutron scattering

The neutron scattering data from the samples and corresponding empty cans were rebinned into energy from time-of-flight histograms, corrected for detector efficiency and normalized to the incident flux. The time-independent background was removed and an absorption correction was performed. The backgrounds from the empty can data were then subtracted. The pixels in each detector were summed, and the detector data were grouped into angle banks of approximately 10° in width from 15° to 135°. The elastic peak was subtracted from the spectrum in each angle bank. For each angle bank, the one-phonon double-differential cross section was isolated using an iterative process. The process begins with a trial one-phonon scattering function to obtain an approximate density-of-states (DOS) and atomic mean-squared displacement. An estimate of the two- through five-phonon scattering is subtracted from the data, and the resulting one-phonon scattering function is used in the next iteration.[15] The final phonon DOS curves were normalized up to 80 meV, ignoring the OH/H_2O modes. Each chemical element has a different neutron scattering cross section, causing an overemphasis of phonon modes where the strongly-scattering atoms have larger displacements. The phonon DOS of Figs. 5 and 6 have not been corrected for this "neutron weighting," because this correction would require full knowledge of the lattice dynamics. Table I presents the results of the quasi-

harmonic vibrational entropies (in units of k_B/atom), which were calculated from the neutron-weighted phonon DOS[16]:

$$S_{vib} = -3k_B \int_0^\infty g(E)[(n_E+1)\ln(n_E+1) - n_E \ln(n_E)]dE, \tag{10}$$

where $g(E)$ is the vibrational DOS and n_E is the phonon occupancy factor. [These results can be converted to molar quantities by multiplying by 8.31 J(mol K)$^{-1}$.] Notice that the largest difference in phonon entropy is only 0.09 k_B/atom, very small on the scale of Fig. 2. While its derivative with respect to x is larger, phonon entropy evidently does not make a substantial contribution to the compositional trend of the entropy of lithiation. On the other hand, the relatively stiff phonons in Li_xCoO_2 do contribute to the negative values of the ΔS of Fig. 2, as discussed below.

D. Electronic structure calculations

The electronic entropy, $S_{el}(T)$, was first calculated from the electron density of states at the Fermi level. Because the thermal energy is relatively small compared to features in the electronic density of states, the electronic heat capacity is linear with temperature. When this heat capacity is used to calculate the electronic entropy by integrating over temperature the ratio of heat capacity to temperature, the result is

$$S_{el}(T) = \frac{\pi^2}{3} g_{el}(\varepsilon_F) k_B^2 T, \tag{11}$$

where $g(\varepsilon_F)$ is the density of states at the Fermi energy, and was obtained from data as in Fig. 7.

The electronic entropy was also calculated from the temperature-dependence of the total electronic energy, assuming a constant $g_{el}(\varepsilon)$. The average of these two approaches is shown in Fig. 8, with the error bars depicting their average difference. The electronic entropy of approximately 0.18 k_B/atom for the metallic phase at $x=0.833$ is expected to decrease to zero in for the insulating phase at $x>0.95$.

The $S_{el}(x)$ in Fig. 8 were fit to a third-order polynomial and differentiated with respect to x to obtain the electronic entropy of lithiation, $\Delta S_{el}(x)$. The resulting $\Delta S_{el}(x)$ is presented in Fig. 9. It is clear that the electronic entropy is too small to play an important role in the lithiation reaction. From the composition dependence of the total energies of the structures, it was possible to calculate the enthalpy of lithiation. These results were generally consistent with the data of Fig. 4.

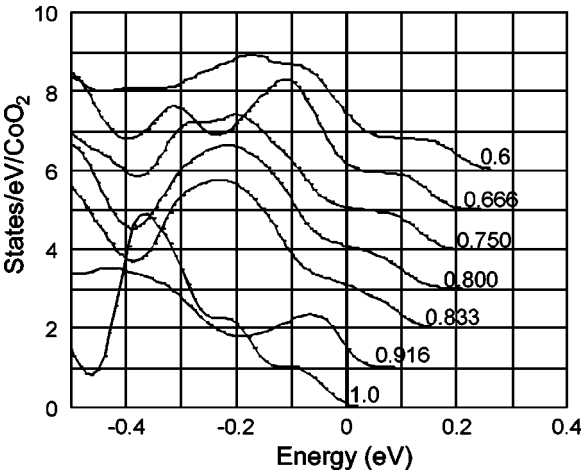

FIG. 7. Calculated electronic density of states of Li_xCoO_2 near the Fermi level. Values of x are given in labels. Curves have been shifted vertically by 1 for clarity.

IV. DISCUSSION

The lithiation reaction proceeds through different phases at different stages.[8,10,17] For the voltage ranges used in our electrochemical measurements, the first reliable observation is at $x=0.58$, where a phase transition occurs between a monoclinic phase at lower x and a layered hexagonal phase of the "O3" structure. This O3 structure of Li_xCoO_2 is best understood as layers of Li atoms intercalated between layers of CoO_2 octahedra. The layered hexagonal O3 phase is reported to be stable in the composition range from $x=0.55$ to 0.75.[8] From $x=0.75$ to 0.93 a phase transition was reported between two layered hexagonal phases with similar lattice

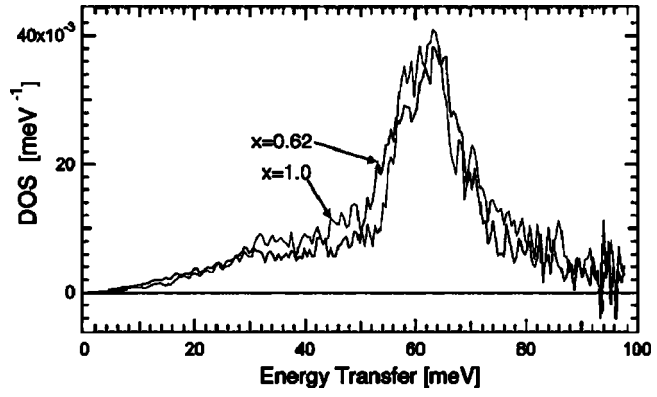

FIG. 6. Neutron-weighted phonon DOS curves of $Li_{0.6}CoO_2$ and $Li_{1.0}CoO_2$.

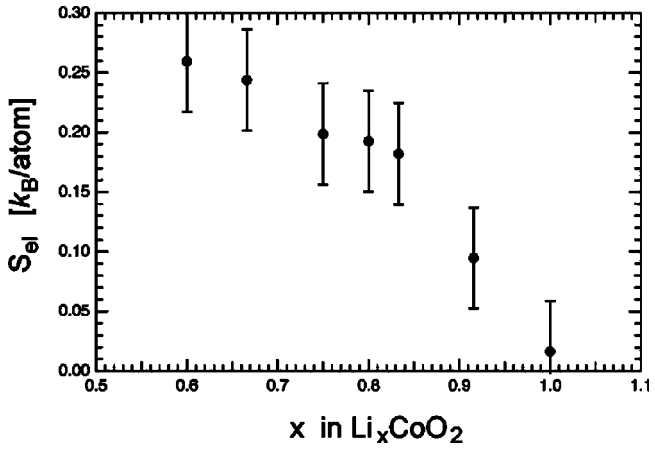

FIG. 8. Calculated electronic entropy of Li_xCoO_2 versus x.

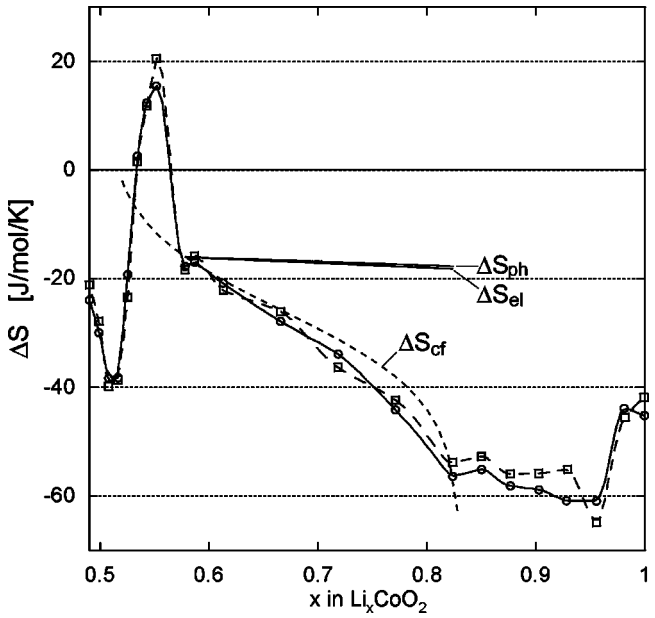

FIG. 9. Configurational entropy (ΔS_{cf}), phonon entropy (ΔS_{ph}), and electronic entropy (ΔS_{el}) contributions to the lithiation reaction in Li_xCoO_2 over the composition range $0.6<x<0.83$, superimposed on the electrochemical data of Fig. 2.

parameters but different electrical conductivity: $Li_{0.75}CoO_2$ is metallic, whereas $Li_{0.93}CoO_2$ is semiconducting. These phases are believed to differ structurally in their arrangement of vacancies on the lithium sites. A disordered arrangement of vacancies is expected in $Li_{0.93}CoO_2$, whereas an ordered structure is expected at the lower lithium concentration. The stoichiometry of this ordered structure is not yet clear. Our data show the boundary of the flat region of the entropy curve in Fig. 1 as being $Li_{0.83}CoO_2$, corresponding to a stoichiometry of $Li_5(CoO_2)_6$. This is consistent with results of Thomas and Newman,[12] who also report a phase boundary quite close to $x=0.83$. It is also consistent with the results from our VASP calculations, and those of Ref. 10, which indicate that the composition $Li_5(CoO_2)_6$ is stable against unmixing into $Li_3(CoO_2)_4$ and $LiCoO_2$. On the other hand, our calculations showed the composition $Li_{11}(CoO_2)_{12}$ to be marginally unstable (by 3 meV per CoO_2 unit) against separation into $LiCoO_2$ plus $Li_{0.833}CoO_2$, consistent with the composition $x=0.917$ being within the two-phase region that we found from the electrochemical measurements. Our electrochemical data show the two-phase region to span the composition range from $x=0.83$ to 0.95, somewhat narrower than reported previously, where the lower concentration was reported to be $x=0.75$ (Ref. 8) or $x=0.8$.[13]

In the composition range from $0.95<x<1.0$, the vacancies on the lithium sites form a disordered solid solution. Placing vacancies on the lithium sites of stoichiometric $LiCoO_2$ therefore causes a rapid decrease of entropy with decreasing x until the composition $x=0.95$ is reached, which is the phase boundary of the disordered solid solution. This is consistent with the observed experimental trend, but the electrochemical data from $0.95<x<1.0$ are not resolved with sufficient detail to warrant a more quantitative comparison with calculation. We performed a more extensive analysis of the entropy of lithiation in the composition range $0.6<x<0.833$, where our experimental data are most reliable.

The neutron inelastic scattering measurements of Figs. 5 and 6 indicated that the phonon entropy did not change significantly with lithium concentration. We estimate that the phonon entropy of lithiation between $x=0.6$ and $x=1.0$ varies by less than 0.5 k_B/atom, making a very small contribution to the compositional trend of the entropy of lithiation. The phonon contribution, labeled ΔS_{ph} on Fig. 9, is therefore shown as a straight line with a small slope. The offset of the calculated entropy of lithiation includes an entropy of the lithium metal counter electrode, as discussed at the end of this section. This contribution should be constant, however, so the vertical height of the calculated $\Delta S_{ph}(x)/\Delta x$ was nominally selected to match the experimental curve at $x=0.6$.

The electronic entropy was calculated from the electron density of states curves of Fig. 7. Evaluations of $\Delta S_{el}(T)$ were performed for different lithium concentrations (Fig. 8) and differentiated with respect to x to obtain the electronic entropy of lithiation, ΔS_{el}. The resulting $\Delta S_{el}(x)/\Delta x$, labeled $\Delta S_{el}(x)$, is presented in Fig. 9. It is clear that the electronic entropy is also too small to play an important role in the composition-dependence of the lithiation reaction. The local density approximation is sometimes unreliable for predicting detailed features of the boundary between occupied and unoccupied states, so it would seem to be at risk for calculating $S_{el}(T)$. In the present case for Li_xCoO_2, however, the difference between the metal and insulating phases is semiquantitatively correct, and prior calculations of the electron energy loss spectra were reliable in the vicinity of the oxygen K and cobalt L transition edges.[18] These successful results on Li_xCoO_2 suggest that VASP results of Fig. 8 are adequate to claim that the electronic entropy of lithiation is negligible, as shown on Fig. 9.

On the other hand, Fig. 8 shows that the metallic phase at $x=0.833$ and the insulating phase at $x=0.95$ should differ in electronic entropy by 0.18 k_B/atom (since the insulating phase should have zero electronic entropy). Assuming an ordered phase at $x=0.833$, which is consistent with the shape of the configurational entropy contribution in Fig. 9, the difference in configurational entropy is almost exactly the same size, 0.20 k_B/atom, but of opposite sign.

The configurational entropy was calculated using Eq. (9) with the composition end point of $x_2=5/6\simeq 0.83$, consistent with the data of Figs. 2 and 4. The lower end point was varied from $x_1=0.0$ to $x_1=0.5$, causing large differences in $\Delta S_{cf}(x)/\Delta x$. For fitting the data of Fig. 2, the most successful compositional endpoint was $x_1=0.5$. The comparison between the configurational entropy for $x_1=0.5$ and the electrochemical results is presented in Fig. 9. The configurational entropy accounts for almost the entire compositional variation of the entropy of lithiation over the composition range from $0.6<x<0.83$, assuming that $x_1=0.5$. It is interesting that the point approximation result of Eq. (6) is so successful. This success indicates that there are only weak correlations between the positions of adjacent lithium atoms in the disordered phase. Evidently 300 K is a high temperature

compared to the ordering or clustering tendencies over most of this range of composition.

Finally we consider the large negative value of ΔS shown in Fig. 2 for the lithium intercalation reaction over the composition range $0.6<x<1.0$. Assessments of the magnitude of this measured ΔS require consideration of the entropy of the counter electrode in the electrochemical cell because the intercalation reaction involves the shrinkage of the metallic lithium electrode. We assume the entropy change of the lithium electrode has no configurational component (it is a pure element), and the electronic entropy is not large (it is a free-electron metal). Inelastic neutron scattering has been performed previously on metallic ^{7}Li, and we compared the reported phonon DOS (Ref. 19) to the results of the present work on Li_xCoO_2. The phonons in metallic ^{7}Li are much softer than those in Li_xCoO_2, consistent with a decrease in entropy when the lithium moves from the metallic lithium anode to the Li_xCoO_2 cathode. A direct comparison of the phonon entropies using Eq. (10) gives a negative phonon entropy of intercalation of approximately -20 J/mol K, somewhat smaller in magnitude than the ΔS measured electrochemically at $x=2/3$ where $\Delta S_{cf}=0$. This difference in phonon entropy is at best semiquantitative, however, because the present neutron scattering spectra were not corrected for the neutron weighting of the phonon scattering by the different elements in Li_xCoO_2. Nevertheless, the entropy of lithiation shown in Fig. 2 may be large and negative because of the difference in the phonon entropy of the anode and cathode.

V. CONCLUSIONS

Measurements of the temperature dependence of open circuit voltages in electrochemical half-cells were used to obtain the entropy of lithiation of Li_xCoO_2 for $0.5<x\leqslant 1.0$. Measured differences in the entropy of the lithiation reaction were as large as 9.0 k_B/atom for the monoclinic phase at $x=0.55$ and the ordered hexagonal phase at $x=0.83$. In the layered hexagonal phase of Li_xCoO_2, the entropy of lithiation decreased by 4.2 k_B/atom from $0.6<x<0.833$.

Three contributions to the entropy of lithiation of the layered hexagonal phase were assessed by experiment and calculation. The phonon entropy, determined from inelastic neutron scattering measurements, was found to make only a small contribution to the measured trend in the entropy of lithiation, but the stiffer phonons in Li_xCoO_2 compared to metallic lithium metal can account for the overall negative values of the entropy of lithiation. The electronic entropy, determined from electronic structure calculations, was found to make small or negligible contributions to the entropy of lithiation. Nearly all of the compositional trend of the entropy of lithiation must originate from the configurational entropy of the distribution of lithium atoms and vacancies on the lithium-bearing planes of the crystal structure. The correct configurational entropy is obtained if lithium-vacancy disorder spans the composition range between the compositions of ordered structures at $x=1/2$ and $x=5/6$.

The composition end point of $x=5/6$ was consistent with electrochemical measurements showing that the two-phase region between metallic and insulating Li_xCoO_2 extends from $x=0.83$ to 0.95, narrower than reported previously. The electronic entropy of the metallic and insulating phases differ significantly, and the changes in the electronic entropy and configurational entropy across the metal-insulator transition are of nearly the same size, but of opposite sign.

ACKNOWLEDGMENTS

We thank A. Van der Ven for kindly supplying atom coordinates for many of the relaxed O3 structures. This work was supported by the Department of Energy through the Basic Energy Sciences Grants DE-FG03-00ER15035 and DE-FG02-03ER15425. The work has benefited from the use of the Los Alamos Neutron Science Center at Los Alamos National Laboratory. LANSCE is funded by US Department of Energy under Contract W-7405-ENG-36. We would also like to acknowledge CNRS for financial support.

[1] L. Anthony, J. K. Okamoto, and B. Fultz, Phys. Rev. Lett. **70**, 1128 (1993).
[2] B. Fultz, L. Anthony, L. J. Nagel, R. M. Nicklow, and S. Spooner, Phys. Rev. B **52**, 3315 (1995).
[3] P. D. Bogdanoff and B. Fultz, Philos. Mag. B **79**, 753 (1999).
[4] G. D. Garbulsky and G. Ceder, Phys. Rev. B **49**, 6327 (1994).
[5] A. van de Walle, G. Ceder, and U. V. Waghmare, Phys. Rev. Lett. **80**, 4911 (1998).
[6] V. Ozolins, C. Wolverton, and A. Zunger, Phys. Rev. B **58**, R5897 (1998).
[7] Y. Nishi, in *Lithium Ion Batteries: Fundamentals and Performance*, edited by M. Wakihara and O. Yamamoto (Wiley-VCH and Kodansha, Tokyo, 1998), p. 181.
[8] J. N. Reimers and J. R. Dahn, J. Electrochem. Soc. **139**, 2091 (1992).
[9] G. Kresse and J. Furthmuller, Phys. Rev. B **54**, 11 169 (1996).
[10] A. Van der Ven, M. K. Aydinol, G. Ceder, G. Kresse, and J. Hafner, Phys. Rev. B **58**, 2975 (1998).
[11] M. Methfessel and A. T. Paxton, Phys. Rev. B **40**, 3616 (1989).
[12] K. E. Thomas and J. Newman, J. Power Sources **119-121**, 844 (2003).
[13] J. N. Reimers, J. R. Dahn, and U. von Sacken, J. Electrochem. Soc. **140**, 2752 (1993).
[14] C. Wolverton and A. Zunger, Phys. Rev. Lett. **81**, 606 (1998).
[15] P. D. Bogdanoff, B. Fultz, and S. Rosenkranz, Phys. Rev. B **60**, 3976 (1999).
[16] D. C. Wallace, *Thermodynamics of Crystals* (Dover, Mineola, New York, 1998), p. 189.
[17] M. Menetrier, I. Saadoune, S. Levasseur, and C. Delmas, J. Mater. Chem. **9**, 1135 (1999).
[18] J. Graetz, C. C. Ahn, R. Yazami and B. Fultz, J. Phys. Chem. B **107**, 2887 (2003).
[19] M. M. Beg and M. Nielsen,Phys. Rev. B **14**, 4266 (1976).